Contents

Chapter 1

Spectral Analysis

One of the fundamental characteristics of Plasma Coagulation Controller for medical applications is what species are produced and deposited during its application. Various studies observed the spectrum of plasma DBD discharge in air at atmosferic pressure and ambient temperature ([1], [2]), it presents peaks relative to reactive species from water, oxygen, nitrogen and its oxides at visible wavelenght, from 200 to 880 nm.

We are intersted in plasma that contains molecules involved in blood coagulation mechanisms, Reactive Oxidant Species (such as hydroxil radical OH) and Reactive Nitrogen Species (derived from nitric oxide NO) ([3]). In this spectroscopy study we give particular attention to them and their precursor, i.e. the presence of transitions relative to hydroxil, oxygen and molecular nitrogen.

1.1 Radiation emission

The source produces plasma from a mixture gas of helium (or neon or argon) and air, along free electrons there are ions and species that collides with energetic electrons, and populate excited or metastable states with short lifetime. All reactive species partecipe in different reactions, and also in excitation and de-excitation reactions with conseguent emission of radiation. When an electron goes from state p at higher energy to state k of lower energy, is emitted radiation with central wavelenght λ_0. Power emitted by this radiation is given by radiant flux $d\phi_\lambda$ and selecting a solid angle as in figure, is possible to define radiance L_λ, and intensity I, as in equations 1.1. Intensity for a radiation ultimately depends on $n(p)$, population density for state p, and Einstein Coefficient for the transition A_{pk} that is typical for the transition ([4]).

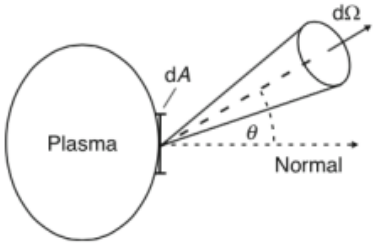

$$\begin{aligned} \lambda_0 &= \frac{hc}{E_p - E_k} \\ L_\lambda &= \frac{d^2\phi_\lambda}{dA\cos(\theta)d\Omega} \\ I &= \int L_\lambda d\lambda = n(p)A_{pk} \end{aligned} \tag{1.1}$$

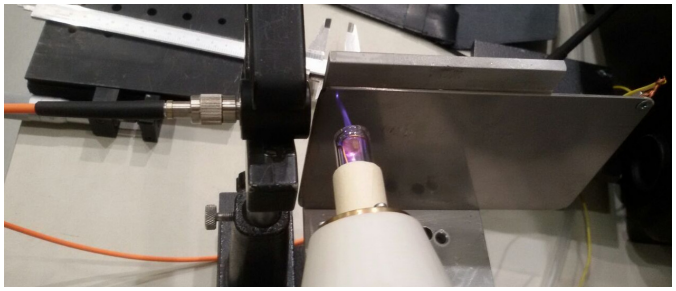

Figure 1.1: Setup of the experiment for line recognitizion: we can see the source, the metal target and the optical setup on the left. Plasma emission is collected by the lens and sent to the spectrometer.

Using air as gas, composed by molecules, reaction that emits radiation in visible wavelenght are vibronic transitions where molecule goes from a vibrational state to another, with a change of vibrational quantum number ν, and/or from a rotational state to another, with change of quantum number J ([5], [6]). When there is a vibrational transition, each line corresponds to different numbers $\nu' - \nu''$, these are transitions well spaced in the spectrum, easy to recognize. Rotational transitions gives birth to bands of peaks not space much, hard to resolve whitout an efficient spectrometer.

There are many reactions involving oxygen and nitrogen (see for example [7]), in this study we determine only principal transition observable with our spectrometer, to know dominant reactive species present in our plasma plume.

The experiments divides in emission line recognition and intensity measurements at different positions and with different gas mixtures.

1.2 Line recognition

We hypotize that plasma emission lines don't depend on which source we use, but on the discharge parameters, as described in chapter **??**, we utilize prototype **A** presented before. A metal plate is positioned as target at a distance of 10 mm from plasma exit, as in figure 1.1. To start the dischare we use helium, with flow set to 2 L/min.

For line recognition we utilize an IsoPlane spectrometer, that separates emissions with different wavelenghts with a grating. The spectrometer has a focal lenght of 320 mm and is equipped with three different gratings: 150, 1200 and 2400 gg/mm, corresponding to different resolutions. As in figure 1.1, light emitted by plasma is collected with a quartz lens and passes trough an optical fiber connected to the spectrometer entry, while at the spectrometer exit there is a CCD camera of 2048 pixels and a count limit of 65 000.

Once a grating is chosen, we can set the start wavelenght on the acquisition system and from there it takes measures until the end of the CCD, for a specific wavelenght interval for every grating. For each measure we select an appropriate acquisition time that allows to observe peaks with a good count number and avoid saturation.

It's important to stress out that, with this measuring method and due to complexity

of plasma reactions and composition, it's not possible to extrapolate quantitative considerations between different species concentration. However it's possible to recognize the presence of certain species and make some considerations watching spectra variation with different experimental setup.

1.2.1 Emission measurements

To see what's generally produced in a discharge we take the spectrum for the entire wavelenght's region intersted, from 230 to 800 nm, with standard discharge paramters: f5 kHz and $\Delta t = 15\,\mu$s. First we do a rapid acquisition with the lowest resolution possible, to see intersting regions and have an idea of required exposition times. After that we do another acquisition with higher resolution for all wavelenghts, measuring several spectra. The entire spectrum is reconstructed attaching different spectra, showed in figure 1.2, where are labelled principal transitions. For every measure wa take also a background spectrum, without plasma, to recognize peaks that are not from the plasma.

We read data with IDL routines ([8]) and analyze it with ROOT *TSpectrum.h* library ([9]). In every spectrum we divide each channel by the exposition time of the spectrum, evaluating the count rate at a specific wavelenght. We estimate white noise contribution as the average value from a portion of the spectrum that doesn't presents peaks, and subtract it to count rates for each wavelenght. In those spectrum we find emission peaks with TSpectrum functions (where is possible to set a treshold in heigth and the general width for lines to be searched) and isolate peaks from background. The exact wavelenght for each transition is found with a gaussian fit in an interval that takes into consideration the asymmetry where it's needed.

As said before, this study is focused on measure related to ROS and NRS, so in lines for NO, OH and N_2.

NO lines We observe two doublets for the transition $A^2\Sigma^+ \rightarrow X^2\Pi$ with vibrational numbers (0-0) and (0-1) ([10], [11]), presented in table 1.1. Intensities for the peaks are normalized with maximum value of 1000 for the acquisition, the table shows as the intensities for this transition is very low. Other transition relative to this molecule have even lower relative intensity and are not observed in our study.

λ [nm]	I [arb.u.]
236.31 ± 0.24	27
237.00 ± 0.15	26
247.02 ± 0.05	28
247.86 ± 0.12	27

Table 1.1: Peaks measured for NO.

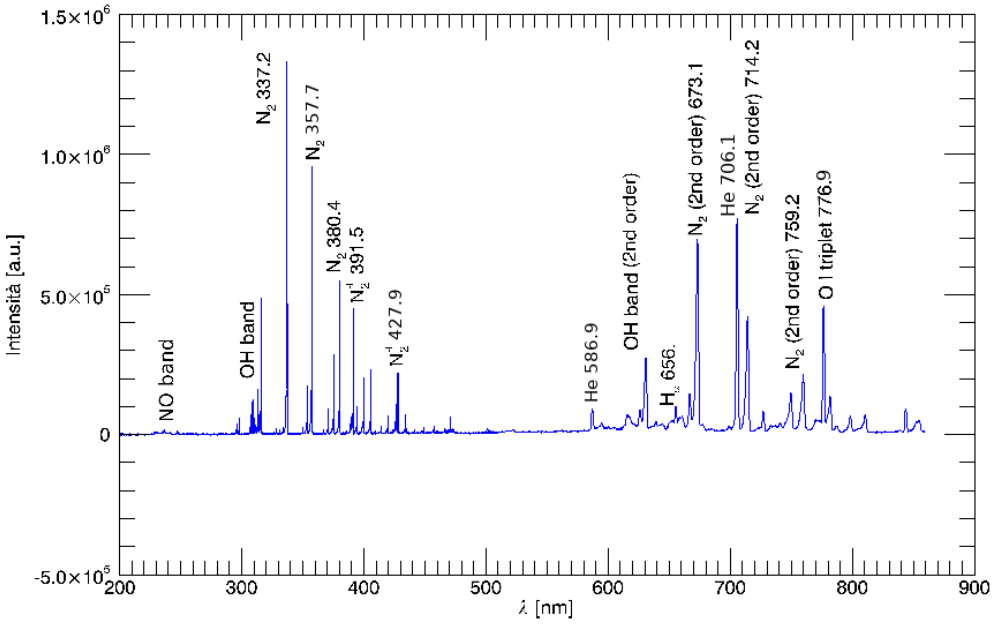

Figure 1.2: Spectrum with an helium flow of 2 L/min, pulse parameters of $f = 5\,\text{kHz}$ and $\Delta t = 16\,\mu\text{s}$. The emission is collected at the end of the nozzle, where plasma exits in air.

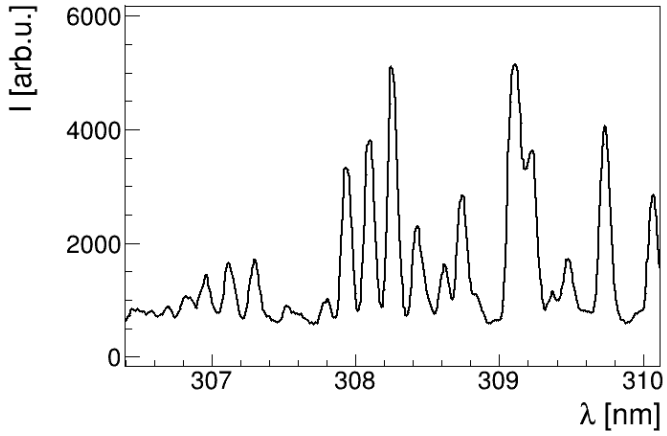

Figure 1.3: Zoom on OH peaks

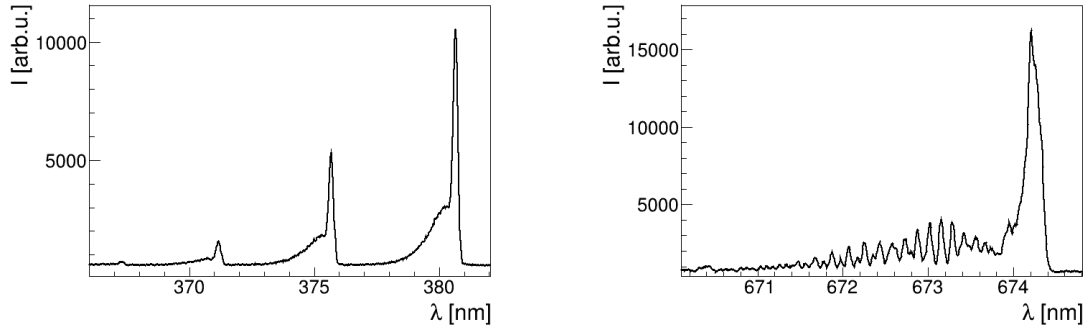

(a) Transitions with $\Delta\nu = 2$ **(b)** Strongest line (0-0), 2^{nd} diffraction order

Figure 1.4: Zoom on N_2 transitions.

OH lines We find the rotational band for transition ($A^2\Sigma$, $\nu' = 0 \rightarrow X^2\Pi$, $\nu'' = 0$), observing 13 principal lines ([12]). In figure 1.3 a zoom on the spectrum, in table 1.2 peak values.

N_2 and N_2^+ lines Measured spectrum presents several lines relative to nitrogen molecules, including the strongest, for diatomic molecule dinitrogen. We observe the Second Positive System for N_2 transition $C^3\Pi \rightarrow B^3\Pi$ and the First Negative System for N_2^+ transition $B^2\Sigma \rightarrow X^2\Sigma$, in table 1.3 peak values ([13], [14]). For N_2 is found also a band of multiple rotational lines centered around $336.58 \pm 0.01\,\text{nm}$. Some of the peaks are seen in the second diffraction order, where there is more distance between lines. In figure 1.4 we presente two zooms for N_2 lines.

Atomic lines We observe other lines from elements present in the plume ([15]):

- $\mathbf{H}_\alpha$ line corresponding to transition from quantum number $n = 3$ to $n = 2$

λ [nm]	I [arb.u.]
306.96 ± 0.01	53
307.11 ± 0.01	58
307.29 ± 0.01	62
307.94 ± 0.01	142
308.09 ± 0.01	148
308.26 ± 0.01	161
308.43 ± 0.01	112
308.62 ± 0.01	46
308.74 ± 0.01	137
309.11 ± 0.01	151
309.22 ± 0.01	120
309.45 ± 0.01	36
309.73 ± 0.01	125

Table 1.2: Peaks measured for OH.

	λ [nm]	I [arb.u.]	$(\nu' - \nu'')$
N_2	316.03 ± 0.01	381	(1-0)
	337.11 ± 0.01	1000	(0-0)
	357.77 ± 0.01	722	(0-1)
N_2	367.22 ± 0.20	58	(3-5)
	371.12 ± 0.04	172	(2-4)
	375.66 ± 0.02	232	(1-3)
	380.64 ± 0.02	423	(0-2)
N_2^+	391.50 ± 0.02	355	(0-0)
	427.45 ± 0.02	180	(0-1)

Table 1.3: Peaks measured for N_2 and N_2^+.

	λ [nm]	I [arb.u.]
H_α	655.96 ± 0.04	113
He	586.94 ± 0.05	122
	705.56 ± 0.01	649
O	776.89 ± 0.01	393

Table 1.4: Lines measured for H, He and O.

- **He** two of the strongest lines for helium
- **O** strong line of oxygen

1.3 Relative intensities

To understand the mechanisms of plasma expulsion and deposition, we measure plasma emission intensity varying voltage peak values, line of sight of the spectrometer and gas composition.

1.3.1 Pulse settings

We measure emission lines with different parameters for the voltage pulse, utilizing the same experimental apparatus as before. As seen in chapter **??** for different pulse repetition rates we have the same electric behavior, but this parameter could still influence species production rates.

We observe spectra with three different parameter combinations, corresponding to different intensity of the treatment:

- low: $f = 5\,\text{kHz}$ and $\Delta t = 15\,\mu\text{s}$
- medium: $f = 10\,\text{kHz}$ and $\Delta t = 10\,\mu\text{s}$
- high : $f = 15\,\text{kHz}$ and $\Delta t = 10\,\mu\text{s}$

For every setting we collect plasma emission along two different line of sight:

- position 1: as close as possible to the end of the nozzle, near plasma exit point from the source;
- position 2: close to the target, at 10 mm from plasma exit point, where it collides with target.

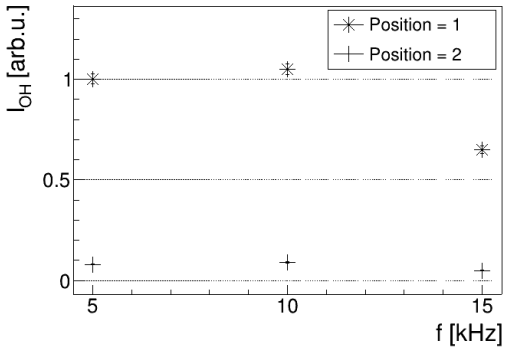

(a) OH intensities in range 306-309 nm

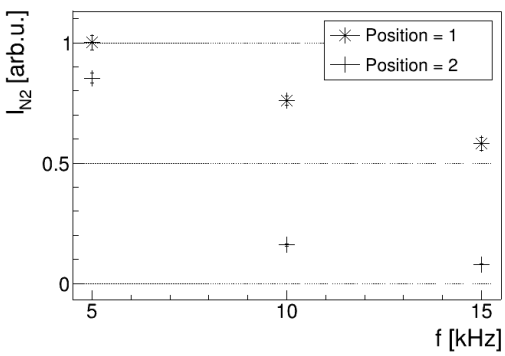

(b) N_2 intensities range 335-337 nm

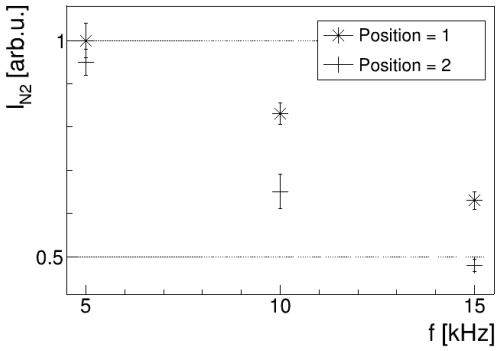

(c) N_2 intensities range 368-382 nm

Figure 1.5: Relative intensities of selected portions of the spectrum, for different pulse repetition rates, for position 1 and position 2.

We evaluate intensities for OH and N_2 species, collectively for the lines in a wavelength range specific for the peaks. For OH lines is considered all the rotational band between 306-309 nm, lines for N_2 are separated in those between 335-337 nm (rotational band and (0-0) transition) and those between 368-382 nm (vibrational transitions with $\Delta\nu = 2$).

In figure 1.5 we present measurements result for considered lines. .

Intensities for OH decreases drastically increasing the distance from the source, in position 2 we find values lower than 0.1% of those from position 1. OH lines for both positions have same intensity with low and medium power setup, while is lower with higher frequency, with similar behavior in both positions.

Also N_2 intensities depend on pulse repetition rate: they decrease with higher pulse rates, for every lines, reaching around 0.6% for $f = 15$ kHz in position 1, and lower values for position 2.

It seems that production of both those reactive species have rates dependant from pulse repetition rates, in particular the intensity of their emission decreases at higher frequencies.

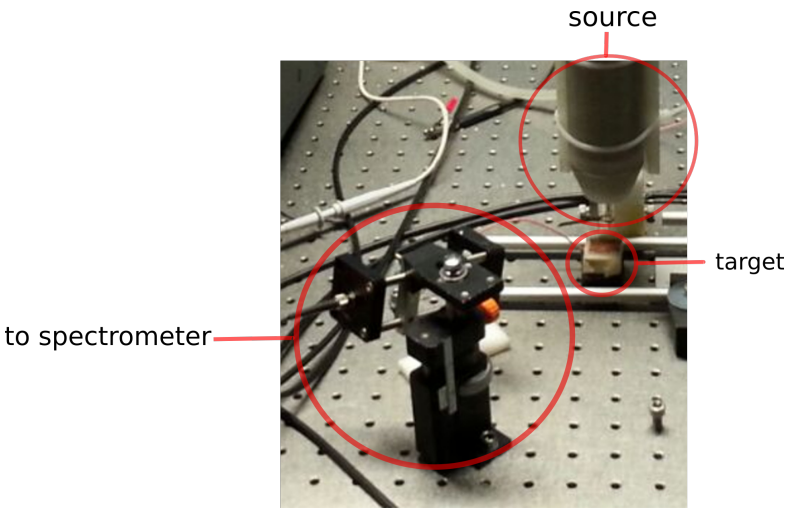

Figure 1.6: Setup of the esperiment for intensity measurements: we can see spectrometer's lens on the left, the source and the metal target.

1.3.2 Line of Sight

We want to analyze plasma emission at different positions with the other source analyzed in this work, prototype **B** in chapter **??**, in a similar way to what we did in the previous measurements. The setup is similar to the one described in chapter **??**: as in figure 1.6, we utilize the glass nozzle and a conductive target at 10 mm from its end.

We utilize a mini-spectrometer *Hamamatsu C10082CAH*, with resolution of 1 nm, spectral range from 200 nm to 800 nm and a CCD sensor *S10420-1106* with 2048 pixels. We find the efficiency of the spectrometer for different wavelenghts with measurements of emission from a lamp with known emission spectrum.

To produce plasma we use three different gasses: helium with a flow of 2 L/min, neon with gas flow 2.5 L/min and argon with flow 2 L/min.

The experimental setup allows to measure plasma emission at different heights along the nozzle axis, we evaluate intensity in four different positions:

- -5 mm, inside the nozzle
- 0 mm, at the end of the nozzle
- 5 mm, between nozzle and target
- 10 mm, right before target position

We consider the total emission for the entire spectral range 200-800 nm and the relative emission for some selected lines, different for the different gasses:

- N_2 : three lines centered at 364.2 nm (transition $(1-0)$), 383.0 nm (transition $(0-0)$) and 403.9 nm (transition $(2-4)$);

- He : one line at 446.2 nm;
- Ne : one doublet at 628.8 nm and 630.6 nm, one doublet at 639.2 nm and 641.0 nm and a single line at 683.1 nm;
- Ar : three different lines at 722.9 nm, 734.0 nm and 772.6 nm.

Results are in figure 1.7. We normalize total intensities to compare emissivity variation for different positions, while relative intensities are divided for the respective total intensity and multiplied for spectrometer efficiency for considered wavelenght. When we use helium to start plasma, emission is lower inside the nozzle, increase at the exit and decreases slightly moving towards the target. For other gasses emission decreases increasing distance from the source. For every gas, emission from N_2 increases until it reaches a constant value. Lines from specific gasses decreases distant from the nozzle, with slope different for different gasses. It's intersting to note how neon emission decreases linearly, while N_2 emission increases and it's an effect that we can see visually: going from the nozzle to the target plasma color goes to red (neon emission) to violet (nitrogen emission).

As we could expect we see that inside the nozzle the emission depends from the gas we use to start the plasma, going outside emission due to nitrogen species becames dominant in the discharge.

1.3.3 Gas composition

We use helium as starting gas, mixed with argon or nitrogen using specific flowmeters, that allows to add up to 0.2 L/min, with resolution of 0.01 L/min. If we set the helium flow to 2 L/min, we can have gas mixtures where argon and nitrogen have a maximum percentage of 10%.

We point the spectrometer at the end of the nozzle and collect spectra for three different gas concentrations, finding the intensities in figure 1.8. When we add nitrogen to the gas, total emission intensity lowers, while nitrogen emission doesn't change as expected. We have this result because we are increasing very slightly nitrogen concentration respect to the quantity naturally present in air, it means that at the end of the nozzle we alredy see all possible nitrogen emission due to molecules naturally present in air. When we add argon, the total emission increases, while relative emission from elements other than argon decreases slightly, as we expect if we add he argon lines to the total sum. It means that the only variation when we add argon is that we see the emission relative to this element, the emission relative to other elements stays unchanged.

1.4 Estimation of plasma temperatures

From diatomic molecule's spectra it's possible to evaluate some parameters that are indicators of plasma's state: rotational temperatures for OH and N_2, T_r, and vibrational temperature for N_2, T_v. These parameters are estimation of the temperature at which

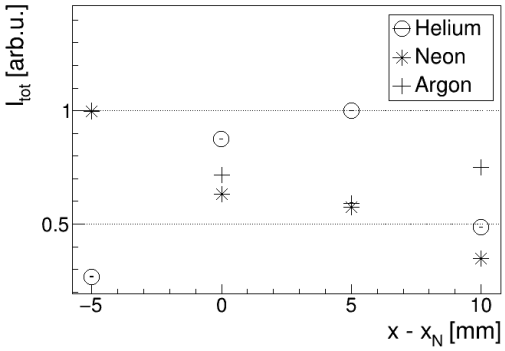

(a) Total emission intensity.

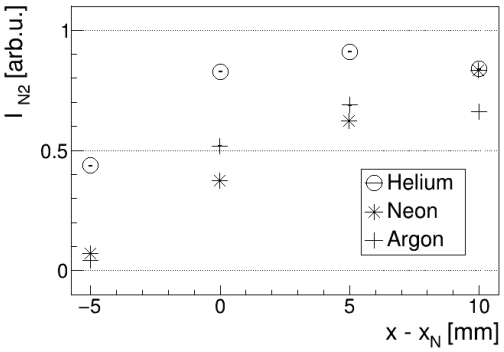

(b) N_2 lines

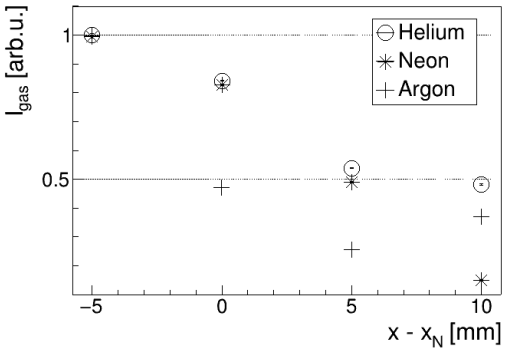

(c) He lines, Ne lines, Ar lines.

Figure 1.7: Behavior of total intensities (a) and relative intensities for selected portions of the spectrum (b-c-d), changing spectrometer's line of sight, with different starting gas. At 0 mm the lens points at the end of the nozzle, at 10 mm at a metal target. Relative intensities in (d) are for lines corresponding to the element that we use as starting gas. Relative intensities take into consideration spectrometer's efficiency and total emission for every position.

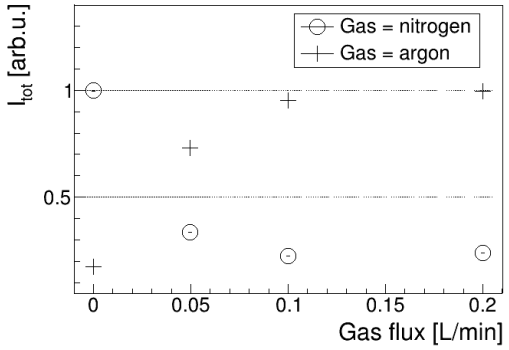

(a) Total emission intensity.

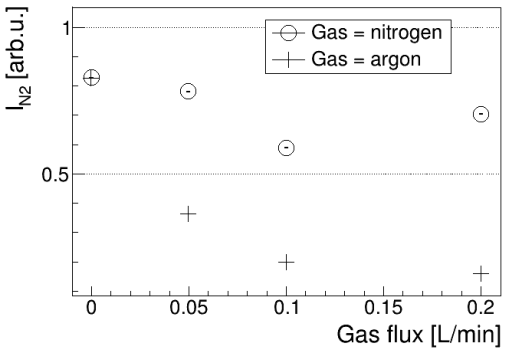

(b) N_2 lines

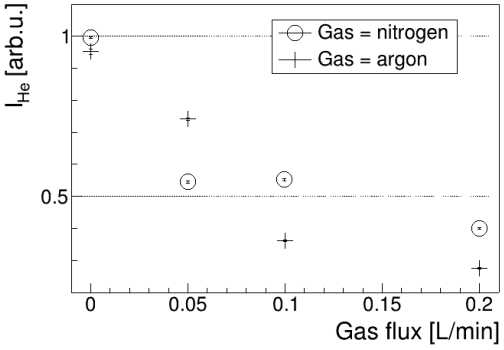

(c) He line

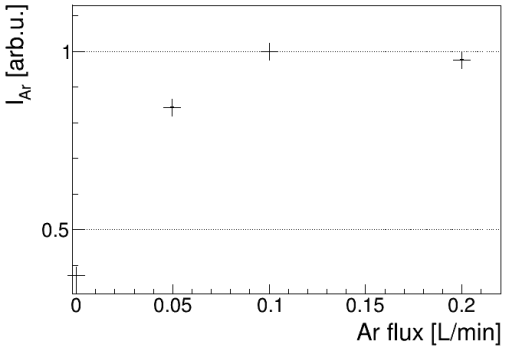

(d) Ar line for argon gas mixture

Figure 1.8: Behavior of total intensities (a) and relative intensities for selected portions of the spectrum (b-c-d-e), changing the composition of the gas. A flow of 0.2 L/min corresponds to the 10% of the total gas flow. Relative intensities take into consideration spectrometer's efficiency and total emission for every gas mixture.

thermal energy is comparable to the gap energy between rotational or vibrational state transitions, they can be defined as in equations 1.2 where ν is the vibrational quantum number and I is the quantizied moment of inertia of the molecule.

$$\begin{aligned} T_r &= \frac{\hbar^2}{2k_B I} \\ T_v &= \frac{h\nu}{k_B} \end{aligned} \tag{1.2}$$

Rotational temperatures can be considered an estimation of neutral gas kinetic temperature. Vibrational temperature gives an idea of the population of vibrational states, useful to determine chemical reactions inside plasma.

1.4.1 Rotational temperature for OH and for N_2

In rotational bands the intensity of a transition for a specific wavelength is proportional to the number density popolation of upper state (equation 1.1), that, considering a Maxwell-Boltzmann distribution, is proportional to the temperature of the species. In equation 1.3 the proportionality is explicitated, with D_0 parameter that depends on number of initial molecules, partition function of the rotational state and quantum rotational numbers for upper and lower state, S is the oscillator strenght specific for the molecule and E_r depends from a constant defined by the vibrational state and from quantum rotational number for upper state ([16]).

$$I = \left(\frac{2\pi}{\lambda}\right)^4 D_0 S \exp\left(-\frac{E_r}{k_B T_r}\right) \tag{1.3}$$

As explained before, rotational bands have many lines, not distinguishable with our spectrometer, an approach to temperature estimation is to simulate spectra with different temperatures and to minimize differences for measured spectrum ([17]). In a predetermined range of temperatures we simulate different spectra with different temperatures, where each line is a gaussian peak with its width that takes into consideration broadning due to thermal motion, Doppler effect and measure resolution. For every spectrum we estimate the mean square difference and select the temperature associated with the minimum differance, while we estimate the error taking an upper and a lower limit where difference is larger by 5% of the minimum value. An example of the spectra is in figure 1.9, while resulting temperatures are in figure 1.10.

From estimated temperatures we can see that they are compatible with each other, for every distance and for every pulse setup. It's then possible to evaluate a mean value for the species, that are $T_{r,\mathrm{OH}} = 352 \pm 38\,\mathrm{K}$ and $T_{r,\mathrm{N_2}} = 321 \pm 41\,\mathrm{K}$, compatible with each other, and that, as said before, can be taken as an indicator of kinetic temperature for neutral species, so as temperature of the fluid. Those temperatures are a little higher then room temperature, but they are compatible with the definition of cold plasma.

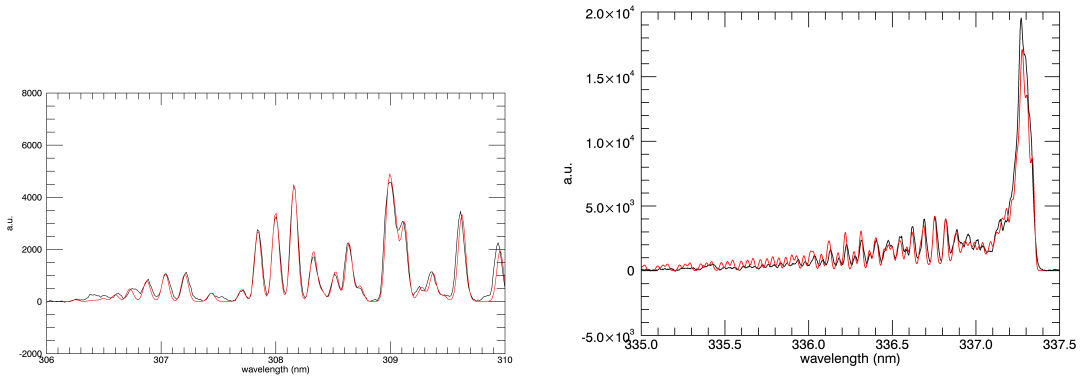

(a) OH **(b)** N_2

Figure 1.9: Example of optimal spectrum simulation for OH and N_2 considered species.

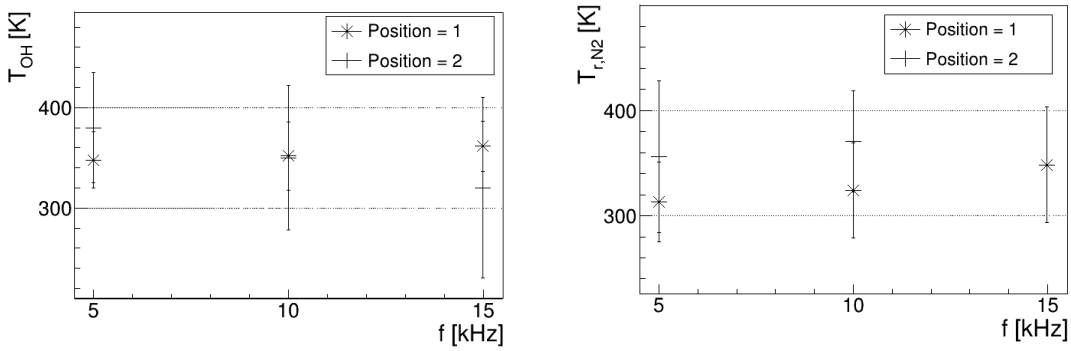

(a) OH **(b)** N_2

Figure 1.10: Estimation of rotational temperature of OH and N_2 molecules, for different parameters setup and positions.

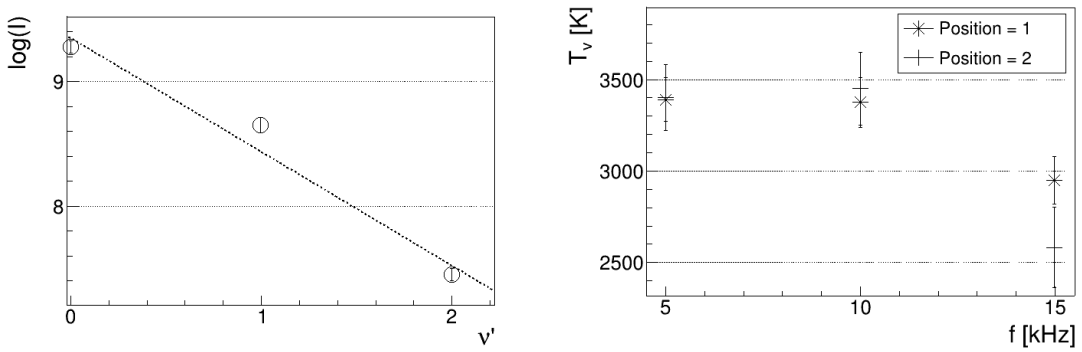

(a) Boltzmann graph for discharge with $f = 5\,\text{kHz}$, $\Delta t = 16\,\mu\text{s}$

(b) vibrational temperature of N_2

Figure 1.11: Example of boltzmann graph for estimation of vibrational temperature (a), for discharge with $f = 5\,\text{kHz}$, $\Delta t = 16\,\mu\text{s}$, lens in position 1 and ibrational temperatures of N_2 molecule (b), for different pulse paramters settings, emission measured from position 1 and 2.

1.4.2 Vibrational temperature for N_2

Given a set of vibrational transition lines with defined $\Delta\nu = \nu' - \nu''$, their relative intensities are correlated to each other, with a proporionality that involves vibrational temperature ([14]). With peak intensities estimated for a given transition, we can made the Boltzmann graph as in figure **??** and evaluate T_v as in formula 1.4.

$$\begin{aligned} log(I(\nu') &= S\nu'' + I_0 \\ T_v[K] &= \frac{10^4}{3.57 \cdot S - 0.03} \end{aligned} \tag{1.4}$$

Results are in figure 1.11. For this parameter we have values compatible with each other at low and medium power pulse settings with a mean value of $T_v = 3405 \pm 154\,\text{K}$, while we find a lower temperature for high power pulse settings $T_v = 2781 \pm 322\,\text{K}$. It seems that whith an higher pulse repetition rate we have lower concentration of excited N_2, produced with lower energy.

Bibliography

[1] Nisha Chandwani et al. "Determination of Rotational, Vibrational and Electron Temperatures in Dielectric Barrier Discharge in air at atmospheric pressure". In: (June 2014). DOI: 10.13140/RG.2.1.2078.6725.

[2] Ioana Gerber et al. "Air Dielectric Barrier Discharge Plasma Source For In Vitro Cancer Studies". In: *Clinical Plasma Medicine* 9 (Feb. 2018), p. 4. DOI: 10.1016/j.cpme.2017.12.006.

[3] S. P. Kuo et al. "Applications of Air Plasma for Wound Bleeding Control and Healing". In: *IEEE Transactions on Plasma Science* 40.4 (2012), pp. 1117–1123. ISSN: 0093-3813. DOI: 10.1109/TPS.2012.2184142.

[4] Hans-Joachim Kunze (auth.) *Introduction to Plasma Spectroscopy*. 1st ed. Springer Series on Atomic, Optical, and Plasma Physics 56. Springer-Verlag Berlin Heidelberg, 2009. ISBN: 9783642022326,3642022324.

[5] Gerhard Herzberg. *Molecular Spectra and Molecular Structure I: Spectra of Diatomic Molecules*. 2nd. D. Van Nostrand, 1950. ISBN: 9780442033859,0442033850.

[6] Wikipedia contributors. *Vibronic spectroscopy*. 2018. URL: https://en.wikipedia.org/w/index.php?title=Vibronic_spectroscopy&oldid=823782704.

[7] I A Kossyi et al. "Kinetic scheme of the non-equilibrium discharge in nitrogen-oxygen mixtures". In: *Plasma Sources Science and Technology* 1.3 (1992), pp. 207–220. DOI: 10.1088/0963-0252/1/3/011. URL: https://doi.org/10.1088%2F0963-0252%2F1%2F3%2F011.

[8] LIAM E. GUMLEY. *Practical IDL Programming*. San Francisco: Morgan Kaufmann, 2002. ISBN: 978-1-55860-700-2. DOI: https://doi.org/10.1016/B978-155860700-2.50003-3.

[9] M. Miroslav. *ROOT documentation for TSpectrum class*. URL: https://root.cern.ch/doc/v614/classTSpectrum.html.

[10] Andre Knie. "Photon induced inner-shell excitation processes of nitrous oxide probed by angle resolved fluorescence and Auger-Electron spectrometry". Dr. Kassel: Univ. Kassel, 2013. ISBN: 978-3862194582.

[11] H.A. Van Sprang, H.H. Brongersma, and F.J. De Heer. "Absolute emission cross sections for the calibration of optical detection systems in the 120–250 nm range". In: *Chemical Physics Letters* 65.1 (1979), pp. 55 –60. ISSN: 0009-2614. DOI: https://doi.org/10.1016/0009-2614(79)80124-4. URL: http://www.sciencedirect.com/science/article/pii/0009261479801244.

[12] C. de IZARRA. "COMPUTER SIMULATION OF THE UV OH BAND SPECTRUM". In: *International Journal of Modern Physics C* 11.05 (2000), pp. 987–998. DOI: 10.1142/S0129183100000857. eprint: https://doi.org/10.1142/S0129183100000857. URL: https://doi.org/10.1142/S0129183100000857.

[13] S. B. Bayram and M. V. Freamat. "Vibrational spectra of N2: An advanced undergraduate laboratory in atomic and molecular spectroscopy". In: *American Journal of Physics* 80.8 (2012), pp. 664–669. DOI: 10.1119/1.4722793. eprint: https://doi.org/10.1119/1.4722793. URL: https://doi.org/10.1119/1.4722793.

[14] N Britun et al. "Determination of the vibrational, rotational and electron temperatures in N2and Ar–N2rf discharge". In: *Journal of Physics D: Applied Physics* 40.4 (2007), pp. 1022–1029. DOI: 10.1088/0022-3727/40/4/016. URL: https://doi.org/10.1088%2F0022-3727%2F40%2F4%2F016.

[15] A. Kramida et al. 2018.

[16] Se Youn Moon and W. Choe. "A comparative study of rotational temperatures using diatomic OH, O2 and N2+ molecular spectra emitted from atmospheric plasmas". In: *Spectrochimica Acta Part B: Atomic Spectroscopy* 58.2 (2003). INTERSIBGEOCHEM 01, pp. 249 –257. ISSN: 0584-8547. DOI: https://doi.org/10.1016/S0584-8547(02)00259-8. URL: http://www.sciencedirect.com/science/article/pii/S0584854702002598.

[17] Charles de Izarra. "UV OH spectrum used as a molecular pyrometer". In: *Journal of Physics D: Applied Physics* 33.14 (2000), pp. 1697–1704. DOI: 10.1088/0022-3727/33/14/309. URL: https://doi.org/10.1088%2F0022-3727%2F33%2F14%2F309.